Nonresonant Surface-Enhanced Raman Scattering of ZnO Quantum Dots with Au and Ag Nanoparticles

Anna Rumyantseva,[†] Sergey Kostcheev,[†] Pierre-Michel Adam,[†] Sergey V. Gaponenko,[‡,*] Svetlana V. Vaschenko,[‡,§] Olga S. Kulakovich,[‡] Andrey A. Ramanenka,[§] Dmitry V. Guzatov,[⊥] Dmytro Korbutyak,[¶] Volodymyr Dzhagan,[¶] Alexander Stroyuk,[#] and Vitaliy Shvalagin[#]

[†]Université de Technologie de Troyes, 12 Rue Marie-Curie BP 2060, 10010 Troyes Cedex, France, [‡]B. I. Stepanov Insitute of Physics, National Academy of Sciences of Belarus, Minsk 220072 Belarus, [§]Belarussian State University, 4 Nezavisimosti Avenue, Minsk 220030 Belarus, [⊥]Yanka Kupala Grodno State University, Grodno, 220023, Belarus, [¶]V.Ye. Lashkaryov Institute of Semiconductor Physics, National Acadamy of Science of Ukraine, Pr. Nauky 45, 03028 Kyiv, Ukraine, and [#]L.V. Pysarzhevsky Institute of Physical Chemistry, National Acadamy of Science of Ukraine, Pr. Nauky 31, 03028 Kyiv, Ukraine

ABSTRACT Pronounced 10^4-fold enhancement of Raman scattering has been obtained for ZnO nanocrystals on substrates coated with 50 nm Ag nanoparticles under nonresonant excitation with a commercial red-emitting laser. This makes feasible beyond 10^{-18} mole detection of ZnO nanocrystals with a commercial setup using a 0.1 mW continuous wave laser and can be purposefully used in analytical applications where conjugated nanocrystals serve as Raman markers. For Au-coated surfaces the enhancement is much lower and the heating effects in the course of Raman experiments are pronounced.

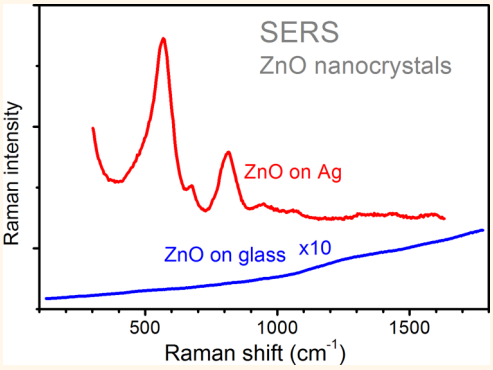

KEYWORDS: SERS · ZnO nanocrystals · plasmonic enhancement

Plasmonic enhancement of fluorescence and Raman scattering has been extensively studied for molecular systems during the last decades[1−3] and is considered as an important driving phenomenon in nanoscience toward ultrasensitive analysis in medicine, forensic, environmental, and cultural heritage research. It occurs owing to local incident field enhancement and local density of states enhancement promoted by generation of localized plasmons and/or surface plasmon-polaritons at nanotextured metal−dielectric interfaces. For surface-enhanced Raman scattering (SERS) extreme enhancement factors more than 10^{10} are reported allowing for single molecules detection. For fluorescence, however, quenching occurs along with the enhancement mechanism, and the overall fluorescence yield rises up typically by an order of magnitude provided an optimal spacing of 5−10 nm from the metal is maintained to prevent nonradiative relaxation of electron excited states. For semiconductor nanocrystals (quantum dots) plasmonic enhancement of photoluminescence has been well established for a decade.[4−6] However, plasmonic enhancement of Raman scattering for quantum dots has not been extensively examined to date. Surprisingly enough, since the pioneering paper in 1993 by Honma *et al.*[7] only a few reports have been published on the matter. These authors reported approximately 10^2-fold enhancement of Raman signal from CdS colloidal nanocrystals mixed with silver colloidal nanoparticles upon resonant excitation of CdS nanocrystals by a blue-green Ar laser (467 nm wavelength). Milekhin *et al.*[8] observed 700-fold increase in Raman intensity for a Langmuir—Blodgett film containing CdS nanocrystals covered with Ag clusters. The excitation wavelengths in the blue-green range corresponded to resonant absorption of CdS dots overlapping with the extinction maximum of silver clusters. An increase of Raman scattering for both resonant and nonresonant excitation was observed for CdSe dots deposited on gold patterned surfaces though enhancement factors are not reported.[9,10] Raman scattering

* Address correspondence to s.gaponenko@ifanbel.bas-net.by.

Received for review January 21, 2013 and accepted March 6, 2013.

Published online March 06, 2013
10.1021/nn400307a

enhancement for quantum dots goes well far beyond basic research since Raman labels have been proposed to substitute fluorescent labels in high-sensitive biomolecule detection in medicine, for example, identification of onco-sensitive markers in bioliquids.[11] Sharpness and specificity of Raman spectra *versus* fluorescence emission spectra promise better recognition and enable multiplexing. Recent successful implementation of ZnS quantum dot Raman labeling of proteins[12] should be noted. In the context of the growing interest in various optical applications of ZnO,[13,14] SERS for ZnO nanocrystals became the subject of active experimental studies. Shah *et al.* reported noticeable enhancement of Raman scattering from ZnO core nanocrystals covered with a silver nanoshell.[15] The excitation source applied was a 325 nm He–Cd laser to enable resonant ZnO excitation. A similar approach to ZnO/Au synthesis with the same type of excitation source yielded 2- and 3-fold increase in Raman efficacy only.[16,17] Recently Milekhin *et al.* demonstrated 10^3-fold enhancement of Raman scattering for surface optical phonon modes with ZnO nanocrystals in Langmuir—Blodgett films covered with silver clusters by vacuum deposition.[18] However, since nanocrystals in films can hardly be applied to biomolecule labeling, these findings are to be extended toward SERS implementation and analysis for colloidal ZnO nanocrystals.

In this paper, we report on substantial enhancement of nonresonant scattering for colloidal ZnO nanocrystals adsorbed on metal films consisting of Ag and Au nanoparticles obtained with the red (632 nm) laser source which is favorable in terms of minor intrinsic photoluminescence excitation in biospectroscopy when quantum dots are considered as promising Raman markers.

RESULTS AND DISCUSSION

Nanocrystals and Substrates. Since the ZnO nanocrystal size (4.5 nm) is comparable with the Bohr exciton diameter, quantum size effect arises manifesting in a pronounced shift of absorption onset toward higher photon energies, that is, shorter wavelengths as compared to the band gap energy of the bulk ZnO in accordance with the data reported in refs 19 and 20. This is shown in Figure 1 in the optical density spectrum, $D = -\log(I/I_0)$ with I (I_0) being transmitted (incident) light intensity,

An example of typical electron microscope image along with the optical density spectrum of a Ag-covered glass substrate is given in Figure 2. Silver nanoparticles are mostly nearly spherical and have an average diameter of approximately 50 nm while a few of them are rod-shaped. The optical density spectrum features typical extinction maximum near 400 nm with a noticeable optical density in the red edge corresponding to the laser wavelength (632 nm) used in Raman

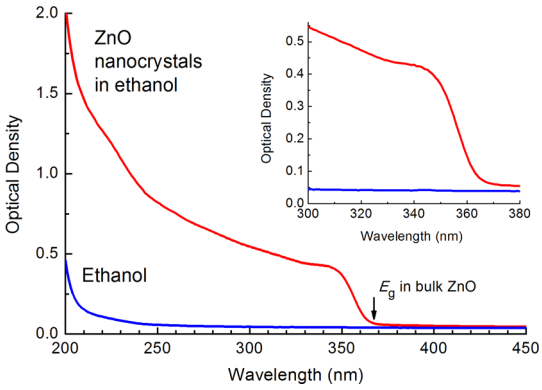

Figure 1. Optical density spectrum of ZnO nanocrystals in ethanol solution in a 2 mm thick cell. The inset shows a portion of spectrum in the narrow range.

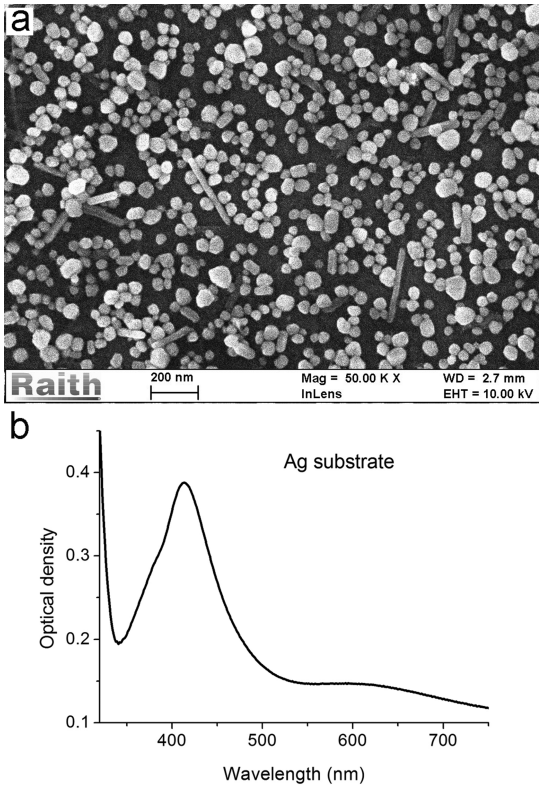

Figure 2. Electron microscope image and optical density spectrum of a glass substrate with deposited silver nanoparticles.

measurements. This red extinction band results either from a small portion of bigger nanoparticles or from nanoparticle aggregates. A shoulder near 400 nm can be tentatively attributed to a quadrupolar mode.

The average diameter of Au nanoparticles was approximately 15 nm as can be seen in Figure 3. The optical density spectrum of Au-coated glass substrate shows a wide extinction spectrum with the maximum close to the laser wavelength applied (632 nm).

SERS with Ag Substrates. At the quantities and concentration of ZnO nanocrystals used in the experiments, no detection of Raman lines is possible for reference

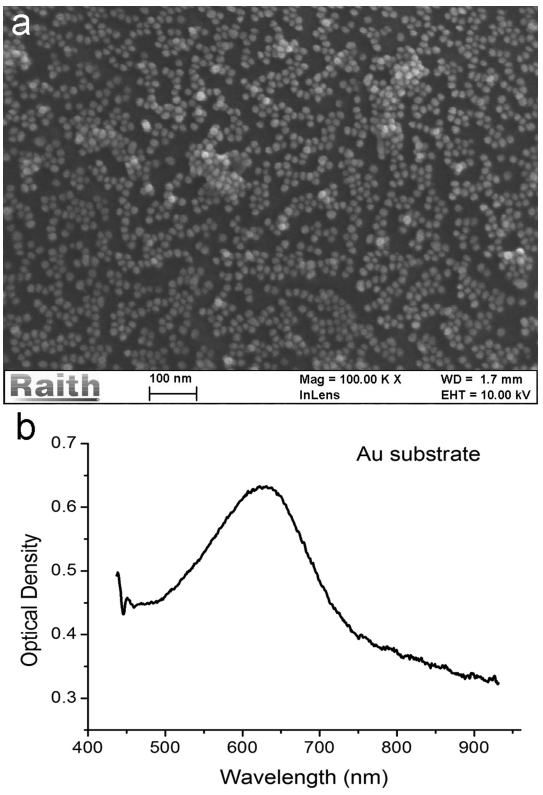

Figure 3. Electron microscope image and optical density spectrum of a glass substrate with deposited gold nanoparticles.

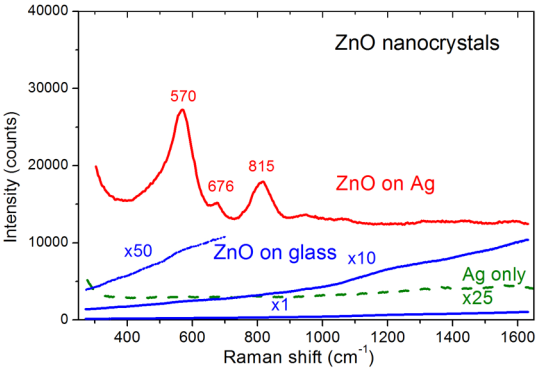

Figure 4. Raman spectrum of ZnO nanocrystals on a silver-coated glass substrate (ZnO on Ag), and the reference spectra for ZnO nanocrystals on silver-free substrate (ZnO on glass) and for silver substrate without ZnO (Ag only).

samples without silver or gold predeposited on glass substrates (Figure 4, curves "ZnO on glass").

In case of silver substrates, Raman signal is enhanced by at least 10^4 times as can be seen from Figure 4 (curve denoted as "ZnO on Ag"). Remarkably, owing to strong enhancement of Raman scattering, silver coated samples showed high intensity with less than 0.1 mW laser power and just 2—5 s acquisition times. The estimated quantity of ZnO involved in the data acquisition is approximately 0.1 femtomole. Taking into account the short acquisition times (5 s) and the low laser power applied (0.08 mW) one can see that the

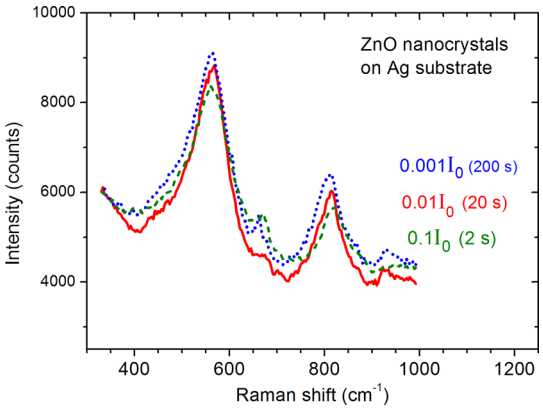

Figure 5. Raman spectra of ZnO nanocrystals on top of silver substrate for various intensity of incident light. I_0 corresponds to approximately 200 kW/cm^2.

detection limit readily goes down to below 0.001 femtomoles for typical commercial Raman microscopes (supposing higher available power and/or longer acquisition times).

Raman spectrum contains a peak at 570 cm^{-1}, a well pronounced peak at 815 cm^{-1}, and an additional less pronounced peak at approximately 676 cm^{-1}. The dominating line at 570 cm^{-1} is assigned to longitudinal optical (LO) phonons. Among the 10 types of optical phonon modes inherent to wurtzite crystals[21,22] only two can be observed in the backscattering geometry employed in our setup. These are E_2-high- (437—444 cm^{-1}) and A_1-LO- (574—579 cm^{-1}) modes.[23] The former typically dominates in Raman spectra of ZnO powders, whereas the latter is the most pronounced mode in thin ZnO films. In our case a low-energy shift of the mode by a few cm^{-1} occurs.

There are a number of reasons that may cause the observed shift: (i) continuous down-ward shift up to more than 10 cm^{-1} due the presence of oxygen vacancies in ZnO lattice;[24,25] (ii) manifestation of interface modes at about 550 cm^{-1} which are not resolved but result in an apparent left-hand asymmetry of the band in Figure 4 and shift of its maximum;[26] (iii) heating of nanocrystals by laser light[27] resulting in a decrease in vibrational frequency because of crystal lattice expansion. Owing to a flat phonon dispersion near the Brilluoin zone center, the effect of phonon confinement is negligible for 4.5 nm large ZnO NCs.[28,29]

The contribution from possible heating in the course of illumination during Raman signal acquisition can be evaluated by varying light intensity applied in the experiments. However, varying intensity within more than 2 orders of the magnitude did not result in any shift of the 570 cm^{-1} line (Figure 5). Therefore low-energy shift of the A_1-LO-mode in the Raman spectrum cannot be related to heating and should be attributed to the presence of oxygen vacancies in the ZnO lattice and/or to manifestation of the surface modes. The latter interpretation is in agreement with

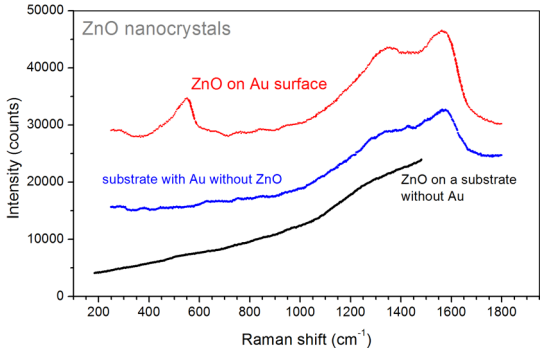

Figure 6. Raman spectra of ZnO nanocrystals on a Au-covered substrate along with reference signals from ZnO nanocrystals on Au-free substrate and from Au-coated substrate without ZnO nanocrystals.

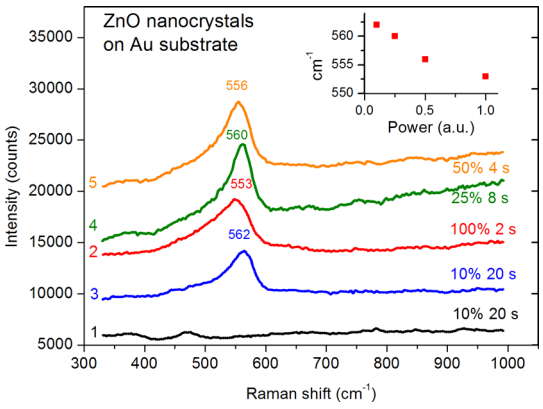

Figure 7. Raman spectra of ZnO nanocrystals on a Au-coated glass substrate for various light intensities indicated in percent. 100% power corresponds to approximately 200 kW/cm^2. Numbering of curves from 1 to 5 corresponds to the order of experimental runs. Spectra aligned vertically for clarity. The inset shows peak position *vs* laser power.

the recent observation of dominating plasmonic enhancement of surface modes in the ZnO nanocrystals.[30]

The pronounced band at 815 cm^{-1} can be treated as a manifestation of surface-enhanced Raman scattering from oxygen complexes on the silver surface. This assignment has been proposed by several groups (refs 30 and 31 and therein). The band is assigned to the O−O stretching vibration of molecularly adsorbed oxygen species. Notably, in our experiments the band does manifest itself only in the presence of ZnO nanocrystals solution deposited on top of the Ag-coated substrates. On a ZnO free portion of Ag-coated substrates no signature of this band can be detected (Figure 4, curve labeled "Ag only"). Therefore zinc oxide nanoparticles are supposed to promote oxygen adsorption on the silver surface.

Possible rationale can be as follows. Being an *n*-type semiconductor, when exposed to ambient air ZnO nanocrystals may adsorb oxygen from air. Oxygen molecules can serve as acceptors to the semiconductor and in the case of an excessive amount of "free" electrons in nanocrystals can form traps for them. Thus a negatively charged surface layer develops. O_2^- molecules can leave the surface only if they lose an electron. Therefore, in our experiments the oxygen groups localized at the ZnO surface exhibit plasmonically enhanced Raman scattering.

SERS with Au Substrates. Surface-enhanced Raman scattering has been also readily observed upon deposition of ZnO nanocrystals on Au-coated glass substrates. The A_1-LO-mode remains to be pronounced, and in many cases it is the only detectable line within the range of 200−2000 cm^{-1} (Figure 6, curve denoted as "ZnO on Au"). In many cases pronounced wide bands near 1300 and 1600 cm^{-1} were also detected These bands were found to be present in the reference samples without ZnO nanocrystals deposited. These bands are assigned to the underneath polyelectrolyte layer which shows (possibly plasmonically enhanced) Raman scattering owing to finite transmission of colloidal Au film. The observed peaks coincide with so-called B- and G-bands of amorphous carbon[32] which in turn may develop to undesirable pyrolisis of the polyelectrolyte during laser light illumination. This looks plausible provided the light intensity in experiments with Au substrates was typically at least 10 times higher than in the case of silver substrates.

Enhancement factors are roughly estimated to be at least 100 times. A more accurate estimate is hard to calculate since the Raman line from ZnO deposited on a Au-free substrate is not detectable for the amount of ZnO nanocrystals used (Figure 6, ZnO on a substrate without Au).

The dominating A_1-LO-line in the case of ZnO nanocrystals exhibits low-energy shift to approximately 553 cm^{-1} *versus* 570 cm^{-1} as has been detected in the case of Ag-coated substrates. Measurements for various intensities of incident light have shown unambiguously that this additional shift results from laser induced heating of ZnO nanocrystals. Since photon wavelength corresponds to the transparency spectral range of ZnO (see Figure 1), nanocrystals cannot be heated by the laser light directly. Therefore it is the presence of light absorbing Au substrate which causes the heating of nanocrystals. Note that enhanced heating of Au nanoparticles by laser radiation is well-known, and has gained wide interest in the context of cancer laser therapy by hyperthermia (photothermal cancer therapy).[33] The monotonic long-wave shift of the A_1-LO-line with rising light intensity is apparent in Figure 7 (curves 2−5 and the inset). In these measurements, the acquisition time has been modified inversely proportional to light intensity to keep the total amount of absorbed energy constant. The sample area has not been subjected to any illumination between Raman signal acquisition runs. The intensity was changed nonmonotonically to exclude possible heat acquisition or other memory-like effects. The results presented in Figure 7 were reproducible for many spots on the same sample.

Similar results indicating a heating-induced shift of Raman lines for ZnO nanocrystals upon laser illumination without metal substrates but under resonant, strongly absorbed by ZnO nanocrystals UV-light have been reported earlier.[27] On the basis of those results, the estimated temperature to cause the observed shift exceeds 700 °C.

An unexpected effect of "memory" or preannealing has been observed systematically for ZnO nanocrystals adsorbed on Au-coated substrates. The enhanced Raman signal can only be detected after at least a few second exposure to the laser light (632 nm wavelength, 8 mW continuous power, 1.5 μm spot diameter). This is demonstrated by comparison of curve 1 with curve 3 in Figure 7. Both spectra are recorded with the same laser intensity and acquisition (*i.e.*, illumination) time but curve 3 was recorded after curve 2, that is, after 2 s exposure of the same spot to the full laser power. We suppose that heating in course of the above preillumination at full power results in removal of the residual solvent and acetate-ion groups promoting closer proximity of ZnO nanocrystals to Au nanoparticles which is necessary for efficient Raman scattering enhancement. The effect is not observed in the case of silver since there is no detectable heating for silver-coated substrates owing to both different size and thermal properties of silver nanoparticles *versus* gold ones (thermal capacity of gold is twice lower than for silver) as well as to lower laser intensities applied in measurements with Ag-coated substrates. The high Raman signals with lower laser intensities in the case of Ag-coated substrates became possible because of stronger Raman scattering enhancement.

Theory. Raman scattering enhancement factor, F_{RS} for an elementary probe dipole located at point **r** in the vicinity of a metal nanobody upon irradiation with light of intensity I_0 and frequency ω can be calculated in terms of the three contributing factors, namely (i) incident field enhancement factor

$$G_I(\omega, \mathbf{r}) = I(\omega, \mathbf{r})/I_0(\omega) \quad (1)$$

(ii) local photon density of states enhancement factor with respect to vacuum DOS $D_0(\omega')$

$$G_{LDOS}(\omega', \mathbf{r}) = D(\omega', \mathbf{r})/D_0(\omega') \quad (2)$$

and (iii) Gersten—Nitzan factor $G(\omega,\mathbf{r})$ which accounts for the contribution of field reflected from a nanobody to polarizability of a probe dipole at small distances (see refs 1, 3, and 34−36 for details). Therefore, the overall enhancement factor can be written as

$$F_{RS}(\omega, \omega', \mathbf{r}) = G_I(\omega, \mathbf{r})G_{LDOS}(\omega', \mathbf{r})G(\omega, \mathbf{r}) \quad (3)$$

Notably, every contributing term depends on orientation of a probe dipole with respect to a nanobody and incident field polarization as well as on the size and shape of a nanobody. To provide a reasonable simplification of this originally rather complicated problem, we restrict ourselves to a single spherical silver nanoparticle and a nanocrystal whose dipole moment orientation is normal to the silver nanoparticle surface. Silver was taken for modeling since superior enhancement up to or even more than 10^4-fold looks rather challenging provided the laser wavelength is well far from the main extinction maximum. It is reasonable to consider feasibility of these high enhancement values within the framework of the current SERS theory.[35,36] In calculations, the ZnO nanocrystal polarizability is taken to be 20 nm^3 in accordance with ref 37.

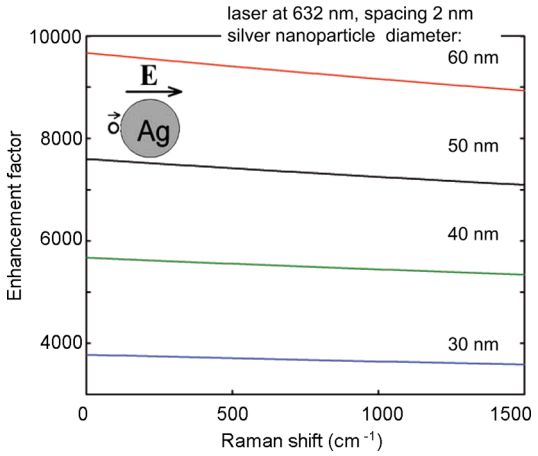

Figure 8. Calculated Raman scattering enhancement factor for a nanocrystal located near a spherical silver nanoparticle for a nanoparticle diameter ranging from 30 to 60 nm.

Calculations were made for a Ag spherical particle, incident field polarization, a quantum dot position, and its dipole moment orientation as shown in the insert in Figure 8. This displacement offers a higher possible enhancement factor. Noteworthy, the theory deals with fixed optimal displacement/orientation of incident light polarization, the dipole moment of a quantum dot, and an axis connecting semiconductor and silver nanoparticles centers. It cannot precisely reproduce the experimental situation with random orientations and spacing as well as probable two-particle, three-particle, and higher metal clusters formation.

From Figure 8 one can see that in the model calculations the enhancement factors of about 10^4 can be reasonably understood with the enhancement factor exhibiting steady growth with nanoparticle size. The latter is important for the development of long-wave extinction, since it is the noticeable extinction value at the laser wavelength which is the primary prerequisite for the observation of every plasmonic enhancement phenomenon in secondary emission, that is, both in spontaneous emission and in scattering of light. In real experiments, size, orientation, and shape distributions as well as random distances of nanocrystals from metal nanoparticles can result in a lower enhancement factor, whereas probable formation of binary, ternary, and higher silver nanoparticle clusters can lead to higher enhancement factors.

CONCLUSION

The pronounced enhancement of nonresonant Raman scattering for ZnO nanocrystals adsorbed on surfaces formed by silver and gold colloidal nanoparticles was observed and examined. The effect was found for the ZnO longitudinal optical phonon line (560−570 cm^{-1}) with a red laser (632 nm), the photon energy of a laser being well below the ZnO absorption onset (350 nm). The enhancement for silver substrates measures up to 10^4 times as estimated for an overall harvested light from 1.5 μm spots. The estimated ZnO detection limit is about 10^{-18} mole. The enhancement for gold substrates is about 10^2 times. In the case of silver substrates a pronounced additional line was detected (815 cm^{-1}), which is assigned to oxygen groups adsorbed from air at the ZnO surface. The results obtained are valuable for application of quantum dot bioconjugates in ultrasensitive detection of biomolecules with quantum dots being Raman markers.

METHODS

ZnO Nanocrystals Synthesis. Colloidal ZnO nanocrystals in ethanol have been synthesized by hydrolysis of zinc acetate (reagent grade) with sodium hydroxide (pure) at 0 °C as has been described recently in detail.[19] After the synthesis colloidal ZnO solution was kept at 55−60 °C for 2 h to promote ZnO particles crystallization. The molar zinc oxide concentration in solution was 0.01 M corresponding to about 10^{-5} M in terms of nanocrystal concentration. The average size of ZnO nanocrystals was approximately 4.5 nm according to measurements by dynamic light scattering and estimations based on the well-documented dependences between the absorption onset position and the size of nanocrystals.

Ag and Au Substrates. To make SERS-active substrates, glass substrates of 1 × 2 cm^2 in size were cleaned by means of ultrasonic treatment in isopropyl alcohol and then kept in a mixture of $H_2O-H_2O_2-NH_3$ (1:1:1) at 70 °C for 15 min. After washing in water, substrates were covered with a polycation layer (PDADMAC, 1 g/L in 0.5 M NaCl) during 20 min to develop a positive charge on a glass surface. Silver and gold nanoparticles were synthesized by a citrate reduction technique of $AgNO_3$[38] and $HAuCl_4$,[5] respectively, so metal particles were negatively charged. Silver nanoparticles were nearly spherical and have an average diameter of approximately 50 nm with only a few of them being rod-shaped. The average diameter of Au nanoparticles was approximately 15 nm. Metal nanoparticles were deposited on PDADMAC-modified substrates by dipping half of the substrate surface in Ag (Au) sol for 24 h. The metal-free remaining portion of the substrate served as a reference sample.

Samples Characterization. The optical extinction of substrates, films, and solutions have been characterized by optical density spectra, $D = -\log(I/I_0)$ with I (I_0) being transmitted (incident) light intensity, using a Cary-500 spectrophotometer (Varian, USA). Electron microscopy has been performed using a Zeiss Geminy instrument.

Raman Spectroscopy Measurements. A 1 μL portion of 0.01 M solution of ZnO nanocrystals was dropped on every substrate and dried for at least 1 h. The portion of solution spread over a few square millimeters on the substrate surface. The reference samples were prepared in a similar way using a portion of glass substrate covered with a polyelectrolyte layer but with neither silver nor gold deposited on top. To ensure stability of the analyte and to check possible side effects, experiments were taken from multiple spots on a surface and were repeated several times during the period of 2 weeks. Raman spectroscopy studies were made using a Jobin-Yvon Labram Raman microscope with a He−Ne laser source (emission wavelength is 632.8 nm), with the full laser power 8.8 mW and a number of attenuating filters used to adjust light power to lower values. The measurements were performed in reflection confocal geometry with a 50^x-objective for sample illumination and the scattered light harvesting. The light spot size at the sample surface was 1.5 μm approximately The typical acquisition times were in the range from 2 to 50 s. All measurements were done with averaging over at least five spectral sets. Remarkably, the data reported in the paper were well reproducible in every case.

Conflict of Interest: The authors declare no competing financial interest.

Acknowledgment. Financial support of NanoMat (www.nanomat.eu) by the "Ministère de l'enseignement supérieur et de la recherche," the "Conseil régional Champagne-Ardenne," the "Fonds Européen de Développement Régional (FEDER) fund," and the "Conseil général de l'Aube" is acknowledged. The work has been also supported by the Republican Basic Research Foundation of Belarus (Belarus—Ukraine joint project), Fund for Fundamental Research of Ukraine (Project No. F40.2/068, F41, 1/017, F40.3/040), and the Alexander von Humboldt Foundation (V. Dzhagan). Additionally acknowledged is a UTT visiting professor grant (S. Gaponenko) as well as the Belarus National Scholarship Programme of the World Federation of Scientists (A. Ramanenka).

REFERENCES AND NOTES

1. Kneipp, K., Moskovits, M., Kneipp, H. Eds. *Surface-Enhanced Raman Scattering*; Springer: Berlin, 2006.
2. Geddes, C. D. Ed. *Metal-Enhanced Fluorescence*; Wiley-VHC: New York, 2010.
3. Gaponenko, S. V. *Introduction to Nanophotonics*; Cambridge University Press: Cambridge, U.K., 2010.
4. Shimizu, K. T.; Woo, W. K.; Fisher, B. R.; Eisler, H. J.; Bawendi, M. G. Surface-Enhanced Emission From Single Semiconductor Nanocrystals. *Phys. Rev. Lett.* **2002**, *89*, 117401.
5. Kulakovich, O.; Strekal, N.; Yaroshevich, A.; Maskevich, S.; Gaponenko, S.; Nabiev, I.; Woggon, U.; Artemyev, M. Enhanced Luminescence of CdSe Quantum Dots on Gold Colloids. *Nano Lett.* **2002**, *2*, 1449–1452.
6. Ozel, T.; Nizamoglu, S.; Sefunc, M. A.; Samarskaya, O.; Ozel, I. O.; Mutlugun, E.; Lesnyak, V.; Gaponik, N.; Eychmuller, A.; Gaponenko, S. V.; *et al*. Anisotropic Emission From Multilayered Plasmon Resonator Nanocomposites of Isotropic Semiconductor Quantum Dots. *ACS Nano* **2011**, *5*, 1328–1334.
7. Honma, I.; Sano, T.; Komiyama, H. Surface-Enhanced Raman Scattering for Semiconductor Microcrystallites Observed in Ag-CdS Hybrid Particles. *J. Phys. Chem.* **1993**, *97*, 6692–6695.
8. Milekhin, A. G.; Sveshnikova, L. L.; Duda, T. A.; Surovtsev, N. V.; Adichtchev, S. V.; Azhniuk, Yu. M.; Himcinschi, C.; Kehr, M.; Zahn, D. R. T. Resonance Effects in Raman Scattering of Quantum Dots Formed by the Langmuir−Blodgett Method. *J. Phys., Conf. Ser.* **2010**, *245*, 012045.
9. Hugall, J. T.; Baumberg, J. J.; Mahajan, S. Surface-Enhanced Raman Spectroscopy of CdSe Quantum Dots on Nanostructured Plasmonic Surfaces. *Appl. Phys. Lett.* **2009**, *95*, 141111.
10. Chursanova, M. V.; Dzhagan, V. M.; Yukhymchuk, V. O.; Lytvyn, O. S.; Valakh, M.Ya.; Khodasevich, I. A.; Lehmann, D.; Zahn, D. R. T.; Waurisch, C.; Hickey, S. G. Nanostructured Silver Substrates with Stable and Universal SERS Properties: Application to Organic Molecules and Semiconductor Nanoparticles. *Nanoscale Res. Lett.* **2010**, *5*, 403–409.

11. Schlücker, S.; Küstner, B.; Punge, A.; Bonfig, R.; Marx, A.; Ströbel, P. Immuno-Raman Microspectroscopy: *In Situ* Detection of Antigens in Tissue Specimens by Surface-Enhanced Raman Scattering. *J. Raman Spectrosc.* **2006**, *37*, 719–721.
12. Chu, X.; Hong, X.; Zou, P.; Men, J.; Liu, Y. Ultrasensitive Protein Detection in Terms of Multiphonon Resonance Raman Scattering in ZnS Nanocrystals. *Appl. Phys. Lett.* **2011**, *98*, 253703.
13. Klingshirn, C. F.; C. F.; Meyer, B. K.; Waag, A.; Hoffman, A.; Geurts, J. M. M. *ZnO: From Fundamental Properties towards Novel Applications*; Springer: Berlin, 2010.
14. Fonoberov, V. A.; Alim, K. A.; Balandin, A. A. Photoluminescence Investigation of the Carrier Recombination Processes in ZnO Quantum Dots and Nanocrystals. *Phys. Rev. B* **2006**, *73*, 165317.
15. Shan, G.; Xu, L.; Wang, G.; Liu, Y. Enhanced Raman Scattering of ZnO Quantum Dots on Silver Colloids. *J. Phys. Chem. C* **2007**, *111*, 3290–3293.
16. Wang, X.; Kong, X.; Yu, Y.; Zhang, H.. Synthesis and Characterization of Water-Soluble and Bifunctional ZnO−Au Nanocomposites. *J. Phys. Chem. C* **2007**, *111*, 3836–3841.
17. Shan, G.; Wang, Sh.; Fei, X.; Liu, Y.; Yang, G.. Heterostructured ZnO/Au Nanoparticles-Based Resonant Raman Scattering for Protein Detection. *J. Phys. Chem. B* **2009**, *113*, 1468–1472.
18. Milekhin, A. G.; Yeryukov, N. A.; Sveshnikova, L. L.; Duda, T. A.; Zenkevich, E. I.; Kosolobov, S. S.; Latyshev, A. V.; Himcinski, C.; Surovtsev, N. V.; Adichtchev, S. V.; *et al*. D.R.T. Surface Enhanced Raman Scattering of Light by ZnO Nanostructures. *J. Exper. Theor. Phys.* **2011**, *113*, 983–991.
19. Stroyuk, O. L.; Dzhagan, V. M.; Shvalagin, V. V.; Kuchmiy, S. Ya. Size-Dependent Optical Properties of Colloidal ZnO Nanoparticles Charged by Photoexcitation. *J. Phys. Chem. C* **2010**, *114*, 220–225.
20. Wong, E. M.; Searson, P. C. ZnO Quantum Particle Thin Films Fabricated by Electrophoretic Deposition. *Appl. Phys. Lett.* **1999**, *74*, 2939–2941.
21. Arguello, C. A.; Rousseau, D. L.; Porto, S. P. S. First-Order Raman Effect in Wurtzite-Type Crysta1s. *Phys. Rev.* **1969**, *181*, 1351–1353.
22. Fonoberov, V. A.; Balandin, A. A. Polar Optical Phonons in Wurtzite Spheroidal Quantum Dots: Theory and Applications to ZnO and ZnO/MgZnO Nanostructures. *J. Phys: Condens. Matter* **2005**, *17*, 1085.
23. Zhu, X.; Wu, H.-Zh; Qiu, D.-J.; Yuan, Z.; Jin, G.; Kong, J.; Shen, W. Photoluminescence and Resonant Raman Scattering in N-doped ZnO Thin Films. *Opt. Commun.* **2010**, *283*, 2695–2699.
24. Fan, H. J.; Scholz, R.; Kolb, F. M.; Zacharias, M.; Gösele, U.; Heyroth, F.; Eisenschmidt, C.; Hempel, T.; Christen, J. On the Growth Mechanism and Optical Properties of ZnO Multi-layer Nanosheets. *Appl. Phys. A: Mater. Sci. Process.* **2004**, *79*, 1895–1900.
25. Pan, H.; Zhu, Y.; Ni, Zh. Optical and Field Emission Properties of Zinc Oxide Nanostructures. *J. Nanosci. Nanotechnol. A* **2005**, *5*, 1683–1687.
26. Fonoberov, V. A.; Balandin, A. A. Interface and Confined Optical Phonons in Wurtzite Nanocrystals. *Phys. Rev. B* **2004**, *70*, 233205.
27. Alim, K. A.; Fonoberov, V. A.; Balandin, A. A. Origin of the Optical Phonon Frequency Shifts in ZnO Quantum Dots. *Appl. Phys. Lett.* **2005**, *86*, 053103.
28. Cheng, H.-M.; Lin, K.-F.; Hsu, H.-C.; Hsie, W.-F. Size Dependence of Photoluminescence and Resonant Raman Scattering from ZnO Quantum Dots. *Appl. Phys. Lett.* **2006**, *88*, 261909.
29. Alim, K. A.; Fonoberov, V. A.; Shamza, M.; Balandin, A. A. Micro-Raman Investigation of Optical Phonons in ZnO Quantum Dots. *J. Appl. Phys.* **2005**, *97*, 124313.
30. Kondarides, D. I.; Papatheodorou, G. N.; Vayenas, C. G.; Verykios, X. E. In Situ High Temperature SERS Study of Oxygen Adsorbed on Ag: Support and Electrochemical Promotion Effects. *Ber. Bunsen. Phys. Chem.* **1993**, *97*, 709–719.
31. Vayenas, C. G.; Bebelis, S.; Pliangos, C.; Brosda, C.; Tsiplakides, D. *Electrochemical Activation of Catalysis Promotion*; Kluwer: New York, 2001.
32. A. C. Ferrari, A. C.; Robertson, J. Interpretation of Raman Spectra of Disordered and Amorphous Carbon. *Phys. Rev. B* **2000**, *61*, 14095–1508.
33. Lapotko, D.; Lukianova, E.; Shnip, A.; Zheltov, G.; Potapnev, M.; Oraevsky, A.; Savitskiy, V.; Klimovich, A. Photothermal Microscopy and Laser Ablation of Leukemia Cells Targeted with Gold Nanoparticles. *Proc. SPIE* **2005**, *5697*, 82–89.
34. Gersten, J.; Nitzan, A. Electromagnetic Theory of Enhanced Raman Scattering by Molecules Adsorbed on Rough Surfaces. *J. Chem. Phys.* **1980**, *73*, 3023–3037.
35. Gaponenko, S. V.; Guzatov, D. V. Possible Rationale for Ultimate Enhancement Factor in Single Molecule Raman Spectroscopy. *Chem. Phys. Lett.* **2009**, *477*, 411–414.
36. Klyachkovskaya, E. V.; Guzatov, D. V.; Strekal, N. D.; Vaschenko, S. V.; Harbachova, A. N.; Belkov, M. V.; Gaponenko, S. V. Enhancement of Raman Scattering of Light by Ultramarine Microcrystals in Presence of Silver Nanoparticles. *J. Raman Spectrosc.* **2012**, *43*, 741–744.
37. Wang, F.; Shan, J.; Islam, M. A.; Herman, I. P.; Bonn, M.; Heinz, T. F. Exciton Polarizability in Semiconductor Nanocrystals. *Nat. Mater.* **2006**, *5*, 861–864.
38. Guzatov, D. V.; Vaschenko, S. V.; Stankevich, V. V.; Lunevich, A. Ya.; Glukhov, Yu. F.; Gaponenko, S. V. Plasmonic Enhancement of Molecular Fluorescence near Silver Nanoparticles: Theory, Modeling, and Experiment. *J. Phys. Chem. C* **2012**, *116*, 10763–10770.